Journal of Applied Polymer Science

Preparation and Gas Transport Properties of Dual-Layer Polysulfone Membranes for High Pressure CO_2 Removal from Natural Gas

Abdul Latif Ahmad,[1] Jimoh Kayode Adewole,[1,2] Choe Peng Leo,[1] Abdullah S. Sultan,[2] Suzylawati Ismail[1]

[1]School of Chemical Engineering, Engineering Campus, Universiti Sains Malaysia, Seberang Prai Selatan, Pulau Pinang, Malaysia
[2]Center for Petroleum and Minerals, King Fahd University of Petroleum and Minerals, Dhahran 31261, Saudi Arabia
Correspondence to: A. L. Ahmad (E-mail: chlatif@usm.my)

ABSTRACT: Permeability, sorption, and plasticization behaviors of dual-layer composite membrane were studied. Polysulfone containing 10.7 wt % glycerol as additive was used for preparing a microporous membrane support. A thin top selective layer was prepared using diethylene glycol dimethyl ether as casting solvent. The overall performance of the membrane was evaluated using Scanning Electron Microscopy, and permeation and sorption tests at pressure up to 50 bar. The prepared membrane displayed high permeability at low pressure which gradually decreased with increase in pressure. Permeability of CO_2 was determined to be 84.97 Barrer at 2 bar. Membrane did not show any plasticization tendency up to the experimental pressure of 40 bar. Plasticization pressure and permeability at plasticization pressure were estimated to be 41.07 bar and 6.03 Barrer, respectively. The improved performance of the membrane is associated to the synergistic properties of the two layers prepared from different formulations of the same polymer. Thus, the dual-layer flat sheet configuration displayed a potential in high pressure CO_2 removal from natural gas. © 2014 Wiley Periodicals, Inc. J. Appl. Polym. Sci. **2014**, *131*, 40924.

KEYWORDS: applications; membranes; oil and gas; plasticizer

Received 24 January 2014; accepted 21 April 2014
DOI: 10.1002/app.40924

INTRODUCTION

Membrane gas separation technology is now of great practical and fundamental interest due to the increasing role of natural gas in the generation of clean energy.[1,2] This technology is now commercially employed in natural gas (NG) processing industry for CO_2 removal from NG. In 2004, membrane market share in CO_2 removal from NG was only about 2%.[3] One of the most important route for expanding the use of membrane technology in gas separation is the optimization of the membrane separation process conditions such as feed pressure. Moreover, CO_2 separation from natural gas components has been reported to be more efficient at high feed gas pressure.[4] However, one of the major challenges of high pressure operations is plasticization phenomenon and low permeability. The economics of membrane gas separation is favorable at high pressure only if the membrane performance remains stable with improved productivity.[5] The maximum pressure beyond which membrane performance becomes unstable is often called a plasticization pressure. This pressure becomes important in practice due to the effect of plasticization phenomenon on membrane selectivity. Membrane with higher plasticization pressure can maintain its selectivity better than membrane with lower plasticization pressure in high CO_2 feed concentration or in high operation pressure.[6]

The emerging trend of penetrant induced plasticization behavior of some natural gas components, such as CO_2 gas, has been noted for quite some time. Also, a number of articles have been presented in the open literature on this subject. One of the most widely investigated glassy polymeric membrane materials for high pressure CO_2/CH_4 separation is polysulfone (PSF). This is due to its commercial availability, low price, chemical stability, mechanical strength, hydrocarbon resistance, good stability, biocompatibility, good toughness, high heat resistance, and ease of processing.[6,7] Both pure and mixed-gas permeation properties of PSF have been extensively investigated[6–14] for asymmetric as well as dense flat sheet. A detailed research work for investigating 11 dense flat sheet polymeric membranes including PSF for high pressure application was done by Bos et al.[15] The plasticization pressure and permeability at the plasticization pressure of these membranes are illustrated in Figure 1.

From this figure, PSF is the most suitable of these membranes for application in high pressure CO_2 removal based on the plasticization pressure (34 bar). Unfortunately, the permeability is

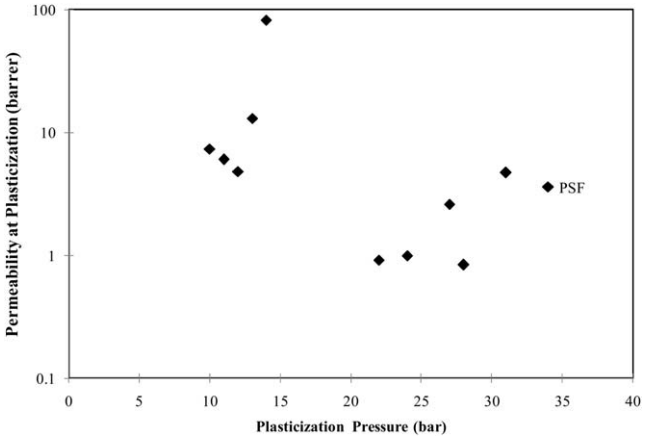

Figure 1. Plasticization pressure of various polymeric membranes and permeability at the plasticization pressure [15].

very low (3.67 barrer) when compared to other polymers that were investigated by the authors. There has been variety of research work on how to improve the permeability of PSF. Results from majority of these works have shown that the permeability can be improved by changing the membrane configurations and use of various solvents and other polymer additives. Aroon et al.[16] carried out extensive study on effects of non-solvents and co-solvents on the morphology and gas permeation properties of PSF asymmetric membranes. Their results revealed that the best formulation is 25 wt % PSF, 10.7 wt % Glycerol, and 64.3 wt % NMP. The membrane prepared from this formulation has permeance of 78.44 GPU for CO_2, 7.66 GPU for CH_4 and a selectivity of 10.24. Scholes et al.[17] investigated the effect of thickness on the plasticization properties of dense flat sheet PSF membranes for high pressure CO_2 removal. Transport properties of the membrane were tested for high pressure behavior using flat polytetrafluoroethylene (PTFE) as membrane supports. The permeability of the membrane at plasticization is between 6.5 and 8.8 Barrer at 35°C depending on membrane thickness. Also, the highest plasticization pressure was reported to be 11.88 bar.

On a general note, the properties of glassy polymeric membranes have been reported to depend on the preparation protocol as well as the casting solvents employed for the preparation.[18–26] Membrane structure can be categorized into two—the physical structure and the chemical structure. The type of casting solvent plays a major role in the nature of physical structure.[24] The effect of casting solvents (cyclohexane, toluene, and THF) on the free volume size distribution of PTMSP membranes was investigated by Bi et al.[24] The authors found that the oxygen permeability through the membranes cast from cyclohexane solutions was almost five times larger than that for membranes from THF solutions. Based on various analysis such as PALS and permeation tests, they then concluded that the improvement on the performance was due to increase in pore size and number density of the free volume. Moreover, solvents have various chemical and physical properties that induce different interactions with polymer chains which then result in different membrane performance responses. Thus, membranes may have solvent-dependent morphologies and separation performances.[21] The effect of the type of casting solvent on the gas permeation properties of an ethylene vinyl acetate (EVA) copolymer was investigated by Mousavi et al.[27] for variety of pure gases. The authors concluded that the casting solvent acts as a transient template which controls the packing density of the final membrane product by covering the polymer molecules with a layer of solvent in the nascent membranes. Investigation on the effect of type of solvent on the morphology and gas separation performance of 6FDA/PMDA-TMMDA copolyimide membranes showed that membranes cast using CH_2Cl_2 or *N*-methyl pyrrolidone (NMP) have an amorphous structure, while film samples cast from *N,N*-dimethyl formamide (DMF) have a crystalline structure. In addition, the gas transport properties of membranes cast from DMF showed the lowest permeabilities for the gases CO_2, N_2, and CH_4.[28] This is despite the fact that DMF has a solubility parameter that is closer to that of the copolyimide used than to those of CH_2Cl_2 and NMP.

Asymmetric and dense isotropic membranes are the most common forms of glassy polymeric membranes used in gas separation. Asymmetric membrane consists of a thin skin layer supported by a porous substructure. The skin layer should be defect free and as thin as possible to provide good flux and permselectivity. It is however very challenging to prepare asymmetric membrane with a defect free and very thin layer. With the dry/wet phase separation technique, asymmetric membrane with defect free effective skin layer in the range 200–1000 Å can be prepared.[26] Simultaneous optimization of the properties of the skin layer and the substructure is however a very challenging task.[29] Moreover, films with thickness <1 μm shows permeation behaviors different from the intermediate thickness (2.5 μm) or thick films.[17,30] Classification of glassy polymers into different regime of behaviors based on their thickness was suggested by Huang and Paul.[31] Plasticization of the thin skin layer of an asymmetric membrane can proceed in a manner that is different from the dense thick films.[26,32,33] For instance, the permeance (P/l) of an asymmetric membrane prepared from polysulfone was reported to increase with increase in pressure whereas the permeabilities of the dense isotropic films prepared from the same polymer decrease with increase in pressure and within the same pressure range. In addition, the permeance of the asymmetric membrane becomes time dependent at much lower pressures than the dense membrane films. Thus, integrally skinned asymmetric membranes are more sensitive to plasticization effects than dense isotropic films.

Dual-layer membrane configuration is one of the techniques that were adopted to further improve membrane performance. Dual-layer membrane consists of a top dense separating layer and a microporous supporting layer.[34–36] Usually, the top layer is of high selectivity and permeability materials in order to provide good permselectivity while the support layer is made from low-cost materials in order to provide the necessary mechanical support for the top layer.[34,37–39] Obviously, the intrinsic property of PSF qualifies it as a good candidate that can be used as both the top and the support layers. One of the problems of the dual-layer is obtaining a delamination-free interface between the top and the supporting layer. The use of compatible materials for dual layer membrane was reported as one of the ways to

reduce the problem of delamination.[36] Using the same materials for both the top and support layers is expected to solve this problem. In addition, the interface between the two layers and between the bulk structures of the inner layers must be porous enough to prevent gas transport resistances which could result in significant decrease in both the permeance and permselectivity of the membranes.[34]

Review of available literature on plasticization resistant polymeric membrane materials revealed that plasticization property is evolving into a conventional trade-off pattern where a membrane exhibiting a high plasticization pressure has relatively low permeability and sometimes low selectivity at the plasticization pressure.[40] Thus the objective of this article is to prepare and investigate transport properties of dual-layer flat sheet membrane in which both the dense selective top layer and the microporous supporting layer are made from PSF. Specifically, we explore the use of a new solvent and a modified dry/wet phase inversion technique to prepare a dual-layer asymmetric composite membrane. To our knowledge, no previous work has been published on the use of diethylene glycol diethyl ether for membrane preparation. Gas separation performance of the membrane at high pressure was evaluated based on the permeability, selectivity, sorption, and plasticization behavior.

EXPERIMENTAL

Materials

Polymer use in this study is Polysulfone (Udel-P1700) (PSF) by Amoco Chemicals. Diethylene Glycol Dimethyether (DEG), 1-Methyl-2-pyrrolidone (NMP), Methanol (MeOH), and Glycerol (GLY) by Merck, CH_4 and CO_2 gases were also used. The PSF was oven dried overnight before being used. Solvent and other organic reagents were used as received. Figure 1(a–c) indicate the chemical structure of the materials used in this article.

Preparation of Membranes

The dense top layer of the membrane was prepared from a solution of 18 wt % PSF in DEG. The solution was then casted on a glass plate and evaporated in an oven at 100°C for 12 h. The membrane was transferred from the oven to a vacuum oven where it was dried on the glass plate for 24 h at 100°C and then peeled with little amount of water. The peeled membrane was then air-dried for several days. The average thickness of the prepared dense membrane was determined as 3.5 μm using Mitutoyo thickness gauge.

The membrane support was prepared by casting a solution comprising 25 wt % PSF, 10.7 wt % Glycerol, and 64.3 wt % NMP on a glass plate. Casted samples were allowed variety of free standing periods of time before being immersed into water and left for 24 h. The free standing periods of time were varied to control the morphology of the membrane support. Membrane sample was later immersed in methanol for 2 h followed by air drying for 48 h. The membrane support was then annealed at 110°C for 36 h under vacuum oven. The dense polysulfone membrane was laminated as a top layer upon the microporous support and the transport properties were tested.

Scanning Electron Microscopy

Membrane microstructure and morphology were examined using scanning electron microscopy (SEM, JEOL JSM-6610L) and field emission scanning electron microscopy (FESEM, Hitachi TM3000). Dried dense top layer and the support membranes were broken in liquid nitrogen and then sputtered with a thin layer of gold. The cross sectional as well as surface morphology of the membranes was examined for both the top layer and the support. Results of morphological tests were used to select the best membrane support samples to be used.

Gas Permeation Measurement

Gas permeability was measured by a constant pressure/variable volume apparatus. The apparatus is composed of the permeation cell, a mass flow controller on the upstream side, and a soap-film bubble flowmeter on the downstream side. The permeation cell was placed in an oven whose temperature was controlled and kept at constant value of 35°C. The active permeation area was 12.25 cm^2.

Permeate flowrate was measured using a bubble flowmeter. At steady-state condition, gas permeability was calculated using the following equation:

$$P = \frac{22,414}{A}\frac{l}{(p_2 - p_1)}\frac{p_1}{RT}\frac{dV}{dt} \quad (1)$$

where A is the membrane area (cm^2), p_2 and p_1 are feed or upstream and permeate or downstream pressures, respectively, R is the universal gas constant (6236.56 cm^3cm Hg/mol K), T is the absolute temperature (K), $\frac{dV}{dt}$ is the volumetric displacement rate of the soap-film in the bubble flowmeter (cm^3/s) and 22,414 is the number of cm^3(STP)of penetrant per mole.[41,42]

In addition, time-dependent permeability was also examined to evaluate the long-term stability of the membrane performance. The time dependence permeability experiment was conducted at 5.8 bar upstream pressure for safety reason.

Gas Sorption Test

Single CO_2 gas sorption tests were performed on the membranes at 27°C using a Gravimetric method up to 50 bar. Sorption parameters (k_D,C'_H, and b) were calculated using the dual sorption model.

$$C = C_{D(\text{HENRY})} + C_{H(\text{LANGMUIR})} = k_D p + \frac{C'_H bp}{1 + bp} \quad (2)$$

where C is concentration and p is the equilibrium pressure of the gas in contact with the membrane. k_D is called the Henry's law coefficient and it characterizes the ease to which polymer chains can open up to accommodate a penetrant gas molecule,- is the Langmuir capacity constant which represents the maximum amount of penetrant gas that can be absorbed into the existing cavities in the polymer matrix, and b is the Langmuir affinity constant representing the affinity of the gas for the Langmuir region. Specifically, these three parameters were obtained by re-arranging the Langmuir portion of eq. (2) as follows:[43]

$$\frac{p}{C_H} = \frac{1}{C'_H b} + \frac{p}{C'_H} \quad (3)$$

The value of K was calculated as

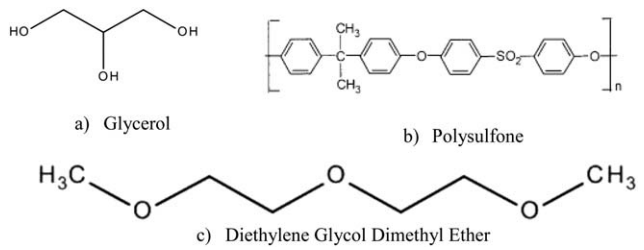

Figure 2. Chemical structure of polymer, solvent, and additive.

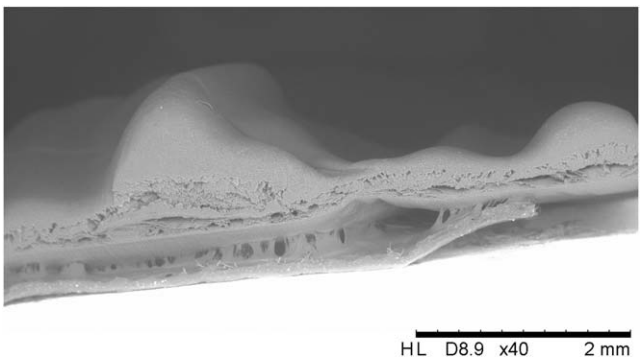

Figure 3. Surface morphology of PSF-support immersed in water after 30 s of free standing time.

$$K = \frac{C'_H b}{k_D} \tag{4}$$

In addition, the sorption coefficient is calculated using eq. (5)

$$S = k_D + \frac{C'_H b}{1 + bp} \tag{5}$$

Estimation of Plasticization Pressure

The permeability–pressure data obtained from the permeation experiment was fitted to a second order equation of the form:[15]

$$P(p) = a_1 p^2 + a_2 p + a_3 \tag{6}$$

Plasticization pressure was obtained by taking the first derivative of eq. (6). Thus

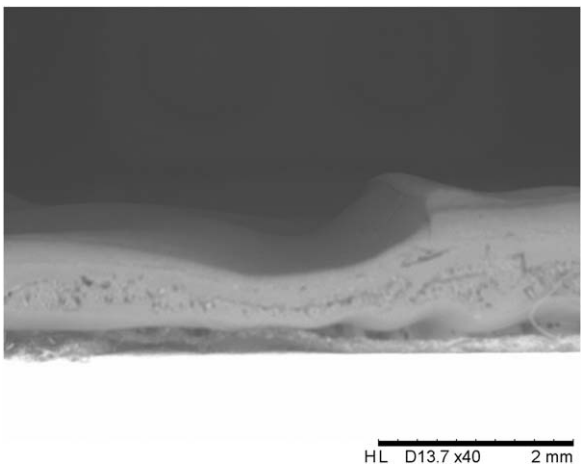

Figure 4. Surface morphology of PSF-support immersed in water after 1 min of free standing time.

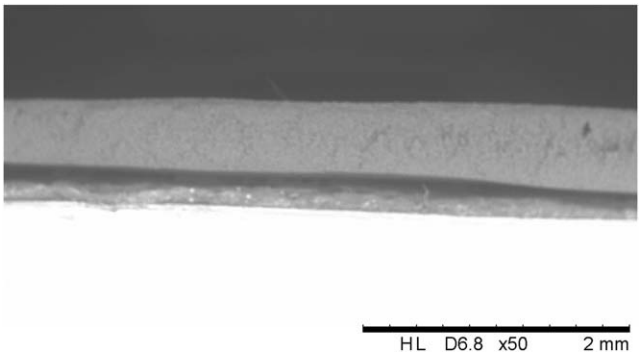

Figure 5. Surface morphology of PSF-support immersed in water after 20 min of free standing time.

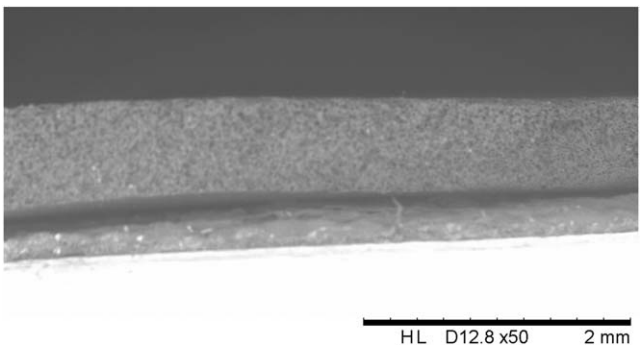

Figure 6. Surface morphology with SEM micrograph of PSF-support immersed in water after 120 min of free standing time.

$$p_l = \frac{-a_2}{2a_1} \tag{7}$$

The permeability at plasticization pressure can then be defined as:

$$P(p_l) = a_3 - \frac{{a_2}^2}{4a_1} \tag{8}$$

where a_1, a_2, and a_3 are constant coefficients.

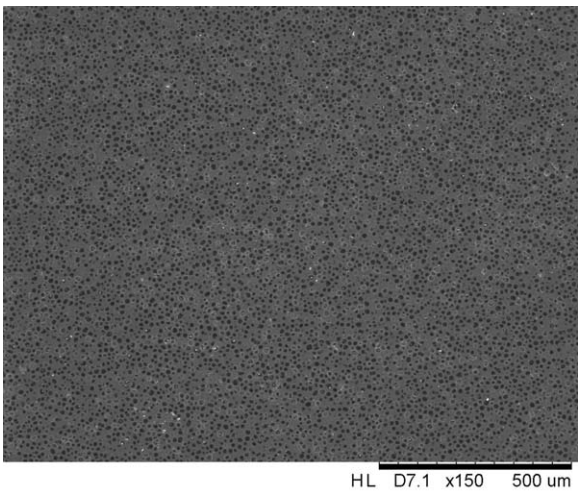

Figure 7. SEM Micrograph of the pore of the support with 20 min free standing time.

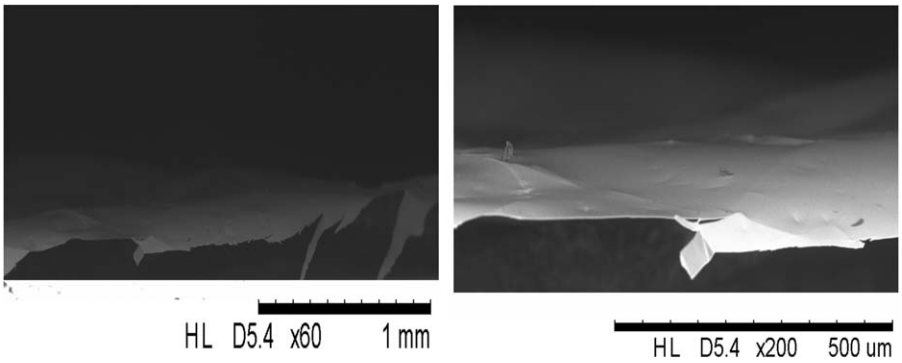

Figure 8. Cross-sectional morphology of the dense PSF top layer at various magnifications.

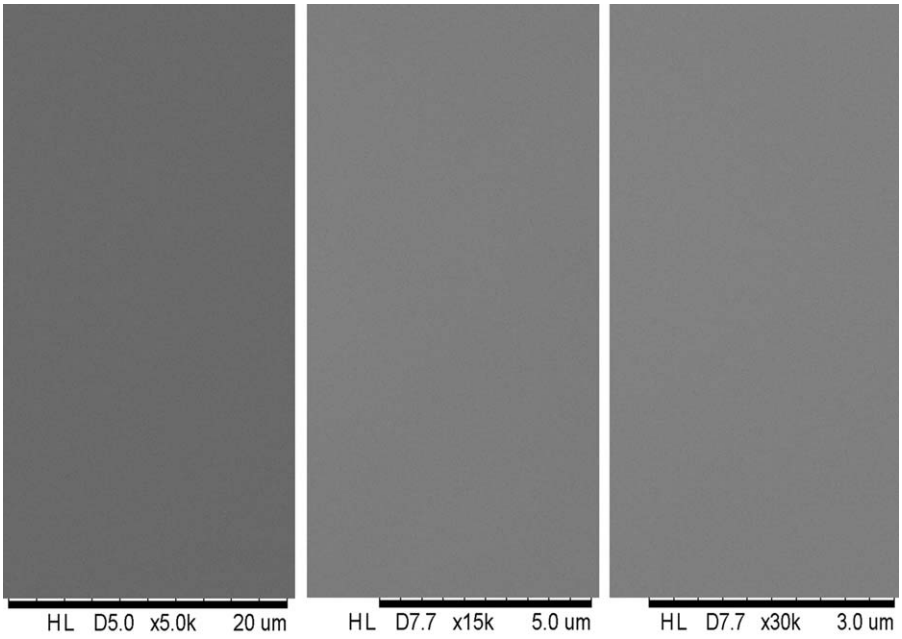

Figure 9. SEM micrograph of the surface of the top layer at various magnifications (a) 5000 times, (b) 15,000 times, (c) 30,000 times.

Quantification of Residual Solvent

Thermogravimetric analysis (TGA) was used to check the residual solvent remaining after drying the membrane. TGA was done from room temperature to 500°C using Perkin Elmer (TGA 7) analyzer at heating rate of 10°C/min under nitrogen atmosphere with flow rate of 20 mL/min using ~10 mg membranes samples. The average boiling point of the solvent used is 160°C. The weight loss between 150 and 170°C was found on the TGA curve. This range of temperature was selected to account for solvent that might have evaporated before the boiling point was reached.

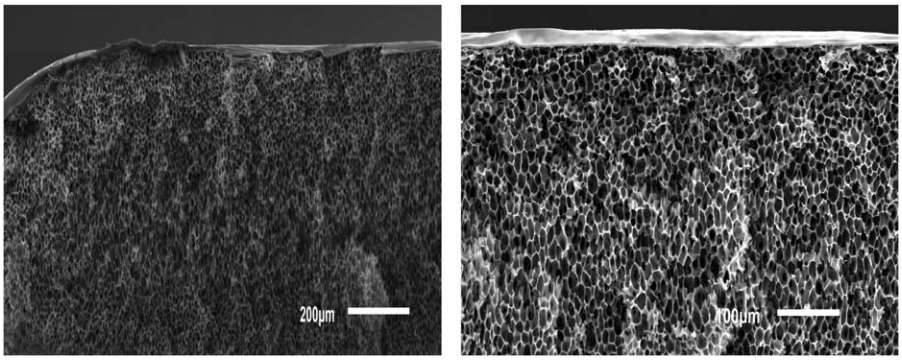

Figure 10. SEM micrograph of composite membrane (the top layer and the porous support): (a) 200 μm, (b) 100 μm.

Table I. Pure CO_2 and CH_4 Permeability of Dense Top Layer Membrane Sample

Pressure (Bar)	P_{CO_2} (Barrer)	P_{CH_4} (Barrer)	Ideal selectivity P_{CO_2}/P_{CH_4}
2.0	84.97	-	-
3.0	45.35	-	-
4.0	34.92	-	-
5.0	29.08	1.258	23.12
5.8	24.57	0.967	25.40
10.0[a]	5.60	-	22.00

[a] Literature value from [11].

RESULTS AND DISCUSSIONS

Scanning Electron Microscopy

Membrane separation performance was known to be directly related to the dope composition from which the membrane has been prepared. A comprehensive study of the relationship has been done by Aroon et al.[16] In this article, dry/wet phase inversion technique was used to prepare the membrane support. Natural convention was used to control the membrane morphology by varying the free standing time (FST) before immersing the membrane into water. The FST was varied from 30 s to 120 min. The best support was choosing based on the surface morphology. SEM micrographs of some of the supports at various FST were shown in Figures 3–7. With low FST, rough undulating membrane surface was formed. This will increase the chances of delamination problem while in operation. Smooth, flat, and defect free surface sample began to emerge at 20 min FST (Figure 5). Up to 120 min, the surface is smooth and defect free (Figure 6).

The observed phenomena can be explained using the membrane formation mechanism and the precipitation path. Membrane morphology and separation properties can be controlled by changing the evaporation time prior to immersion in the coagulant bath, demixing time, and the precipitation path during membrane preparation using the dry-wet technique.[16] Dope

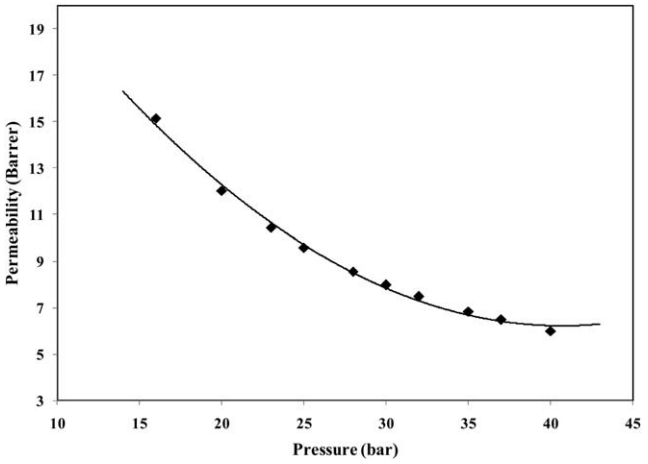

Figure 11. Permeability of dense top layer as a function of upstream pressure.

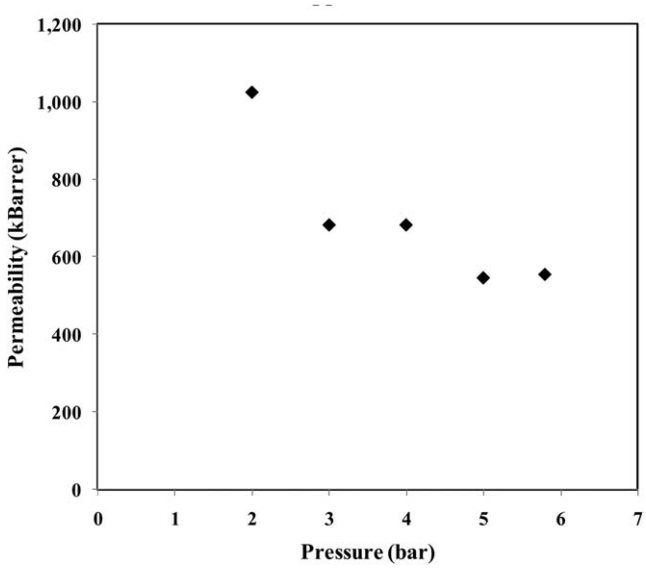

Figure 12. Permeability of the porous support as a function of upstream pressure.

used for preparing the support contains polymer (PSF), solvent (NMP), and a weak non-solvent additive (glycerol). The absence of a volatile solvent, forced convection coupled with the use of a less volatile solvent made the solvent evaporation rate to be very low which consequently affected skin layer formation. During the preparation, membrane immersion was delayed to allow for the saturation of the membrane surface by the high boiling point solvent used. This allowed for instantaneous demixing as soon as the membrane was immersed into water. The resulting membrane thus has a porous top layer as indicated in Figure 7. Another explanation can also be taken from the solvent ratio (which is defined as the ratio of the less volatile to the more volatile solvent). It has been reported that thinnest skin layer is obtained when membrane is prepared from a solution with a high solvent ratio and that such skin layers are usually highly porous. In the dope used for preparation of this support, the solvent ratio was at its maximum due to the absence of volatile solvent. As a matter of fact, the only additive is the glycerol which is also non-volatile.

SEM images of the cross-section and the surface of the top-layer at various magnifications are shown in Figures 8 and 9. The thin cross section of the top layer was clearly revealed by the micrograph in Figure 8. The SEM images of the top layer surface displayed in Figure 9 revealed a continuous defect-free top layer. SEM micrographs of the cross section of the assembled composite were shown in Figure 10 at 200 and 100 μm. The figure reveals two distinct morphologies for the top layer and the porous support. The micro-structure of the support was in the form of a spongy-like uniformly distributed pores with no finger-like macrovoids. Also, the figure reveals no observable delamination at the interface between the top layer and the support.

Gas Permeation Measurement

The overall objective of this article is to evaluate the performance of the membrane for CO_2 removal at high pressure. In this

Table II. Plasticization Pressure, Permeability, Solubility, and Diffusion Coefficient at Plasticization Pressure of Various PSF Membranes

p_l (bar)	$P(p_l)$ (Barrer)	$S(p_l)$ cm^3 (STP)/cm^3	$D(p_l) \times 10^8$ (cm^2/s)	t (μm)	Reference
34.0	3.6	1.4	2.6	32	[15]
11.88	7.5	-	-	2.0	[17]
>40.0	5.99	2.07	2.17	3.5	This work

P_l plasticization pressure, $P(p_l)$ permeability, $S(p_l)$ sorption coefficient, $D(p_l)$ is diffusion coefficient at plasticization pressure, t thickness of the membranes.

regards, permeability and sorption tests were performed on the membrane at pressure up to 50 bar. Permeability test was first performed for both CO_2 and CH_4 at pressure between 2 and 6 bar using a low pressure permeability set up. The performance of the membrane was observed to be slightly unstable at low pressure (<2 bar). A high permeability values of ~85 barrer was obtained for CO_2 while no flow of CH_4 gas was observed at 2 bar for about 1 h of CH_4 exposure. Thus, results obtained for pressure from 2 bar and above were more reliable and that is why the tests were performed within this pressure limit for both gases. Investigation into the reason for this behavior is beyond the scope of this article since our interest is on high pressure operations. The high pressure permeability and sorption tests were performed for pure CO_2 so as to evaluate the plasticization property of the membrane. Results obtained are displayed in Table I and Figure 11. Table I contains the results for the permeabilities of CO_2 and CH_4 and the ideal selectivities from this study and that from literature.[11] The permeability of CO_2 was observed to decrease with increase in pressure from 2 to 5.8 bar. This is typical of the behaviors of glassy polymers in the absence of plasticization phenomenon.[11] For CH_4, permeability is almost zero at pressure between 2 and 4 bar. This means that the membrane selectivity is very high (infinite) at that pressure. The selectivity of the membrane is slightly higher than that reported in the literature for dense polysulfone membrane.

Figures 11 and 12 show the results of CO_2 permeability as a function of pressure for both the dense top layer and the porous support, respectively. The gas permeation of the support was conducted to examine the effect of its resistance to gas permeation at high pressure. As it was observed from the results of the morphology, the permeability of the porous support is higher than that of the top layer by about ten thousand times at a feed pressure of 2bar. It is therefore expected that the support will present no resistance to gas permeation even at high

Table III. Estimated Plasticization Pressure

Experimental		eq. 7	eq. 8	
p_l (bar)	$P(p_l)$ (Barrer)	p_l (bar)	$P(p_l)$ (Barrer)	Reference
34.0	3.6	32.83	3.67	[15]
>40.0	5.99	41.07	6.03	This work

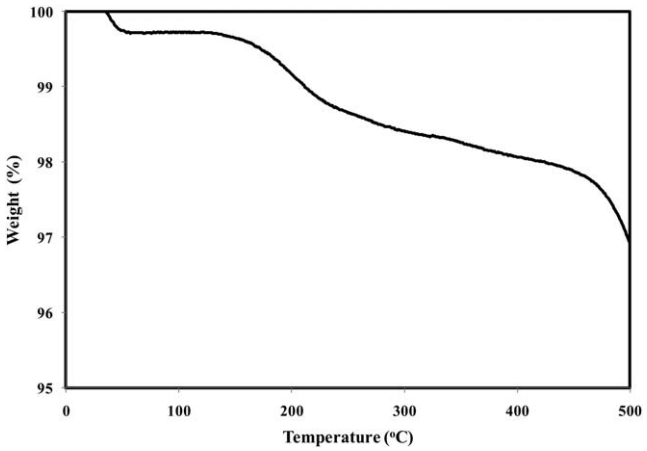

Figure 13. TGA of dense top layer of the membrane.

pressure. The top layer membrane did not show any sign plasticization up to a pressure of 40 bar. At this pressure, the permeability is about 66% higher than the value that was reported in the literature (Table II). The straight line is a second order fit of the permeability–pressure data. The difference in both the plasticization pressure and the permeability at this pressure can be associated to the membrane configuration used. The synergistic effect of using a membrane support containing a polar ether oxygen functional group (Figure 2c) with high affinity for CO_2 and a thin top dense layer is the major contributor to this improvement.[9] Also, the presence of this non-solvent glycerol additive induced instantaneous demixing which in turn lead to better permeability.[16] In addition, the solvent used also has functional group reported to possess very high affinity for CO_2. Although, one would expect that all the solvent must have been evaporated, but their presence before evaporation always leave some effects on the properties of the membranes.[21,24,27,28]

In this article, TGA was used to quantify the residual solvent remaining in the membrane after drying. The result obtained from the TGA is shown in Figure 12. The weight % change between 150 and 170°C was calculated to be 0.131 wt %. This is lower than the recommended limit.[20,44] Thus, the improved performance cannot

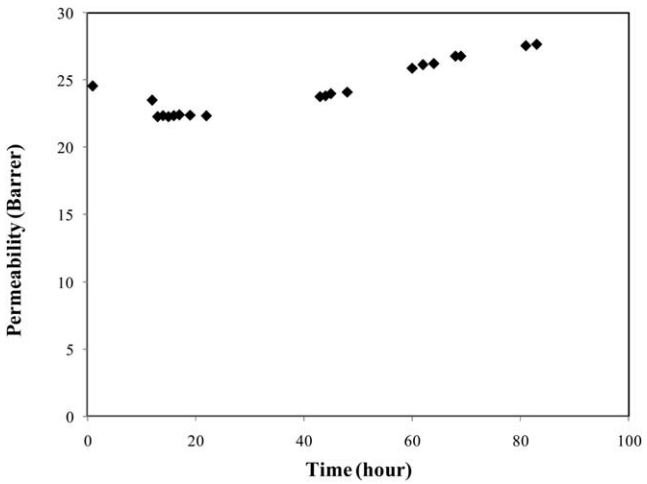

Figure 14. Time dependency of the permeability.

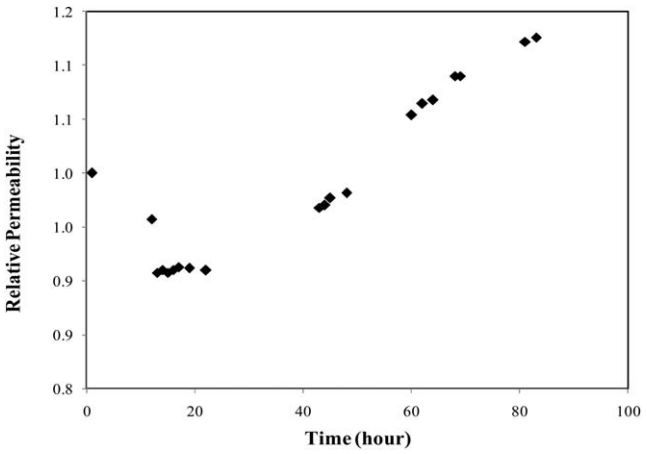

Figure 15. Relative permeability as a function of time.

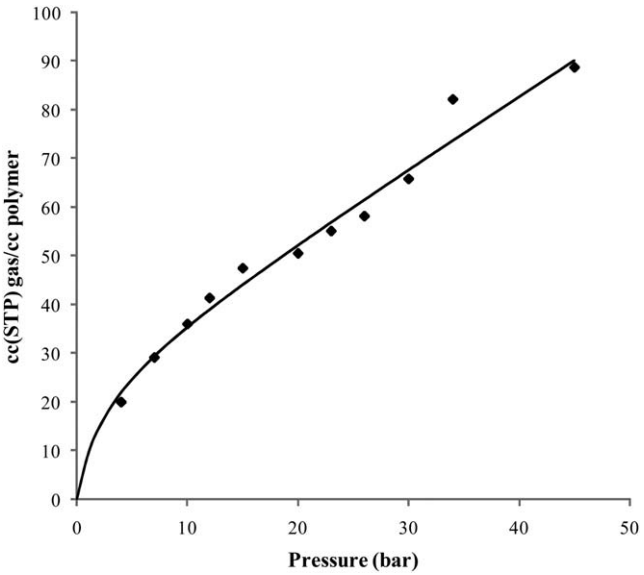

Figure 16. Measured and modeled CO_2 sorption isotherms.

be attributed to the presence of residual solvent. Solution casting method was used to prepare the thin top layer of the dual-layer using DEG. Several attempts were made to apply this same method to prepare top layers using other commonly used solvents such as 1-Methyl-2-pyrrolidone(NMP), *N,N*-Dimethylformamide (DMF), and *N,N*-Dimethylacetamide (DMAc) in order to compare their permeabilities with the DEG membrane. All the attempts were not successful because the resulting membranes contained some surface defects. The lowest defects free thickness that was successfully prepared was about 25 μm. Permeability properties of membrane of such thickness could not be compared with DEG membranes whose thickness is 3.5 μm. Another important factor that is apparent from the contents of Table II is the influence of membrane thickness. Comprehensive research work has already been done by Scholes et al.[17] on CO_2-induced plasticization behavior of ultra-thin polysulfone membrane. The results showed that plasticization pressure increase with increase in membrane thickness. This explains one of the reasons why the plasticization pressure of the dual layer membrane with top layer of 3.5 μm is higher than that of 2.0 μm. On another note, thermal post treatments of membrane have been reported to increase membrane resistance to plasticization.[43,45,46] Both the top layer as well as the support was subjected to thermal treatment. The support was thermally treated at 110°C under vacuum for 36 h while the top layer was annealed at 100°C under vacuum for 24 h. The sorption coefficient was also observed to be about 48% higher compared to literature value. This shows that the enhanced performance was mainly from the improvement in the gas solubility of the membrane. Ideally, the lower thickness of the top layer, the additive and mode of preparation of the support are said to have contributed in the increased permeability and solubility. The heat treatment of the support is one of the factors said to be responsible for the higher plasticization pressure. Plasticization pressure and permeability at the pressure estimated using eqs. (7) and (8) are shown on Table III. The estimation was first done for previously reported data before being applied to the data obtained in this article. The estimated values obtained correlate well with the experimental values. The percentage errors are 3.55 and 1.89% for p_l and $P(p_l)$, respectively.

To investigate the time dependency of the membrane, it was kept to run at 5.8 bar for 83 h. There was a little decrease in the permeability after 12 h and after which the permeability became steady (Figure 14). The little decrease in permeability as observed in this studied is often attributed to variety of reasons which include polymer aging, absorption of impurities, and membrane compaction.[47–49] In this article, the effects of aging and presence of impurities are ruled out since the membrane was subjected permeation tests soon after it was prepared using

Table IV. Dual-Mode Sorption Parameters for Dense Top Layer Compared with Values from Literature

	Numerical value					
Parameters	This work	a	a	b	c	d
$k_D(cm^3(STP)/cm^3bar)$	1.463	0.728	1.25	0.69	0.801	0.631
$b(bar^{-1})$	0.419	0.26	0.155	0.42	0.38	0.313
$C'_H(cm^3(STP)/cm^3)$	25.641	19.6	46.8	11.5	26	29.78
$K(-)$	7.3503	7	5.8032	7	13.308	14.772

a. [12]
b. [52]
c. [17]
d. [10]

high purity CO_2. Thus, the decrease can be attributed to membrane compaction which was later suppressed by the increase in CO_2 concentration within the membrane with time. Detailed investigation of membrane compaction in gas separation is usually studied using the Ultrasonic Time-Domain Reflectometry (UTDR).[49] This test was not performed in this article. The decrease in permeability was later followed by a slow increase after 43 h. The time-dependent behavior of the membrane can further be evaluated by plotting the ratio of permeabilities at various times against the pressure as shown in Figure 15. All permeabilities at time t, $P(t)$, are normalized by the permeability determined after 1hour (i.e., $P_{initial}$). In this figure, there was a sharp drop in the relative permeability before a steady state was achieved (Figure 15). A slight increase in relative permeability was observed at the 43rd hour. This is not due to plasticization since the plasticization pressure was confirmed to be far above 5.8 bar. This increase was 11.43% after 83 h. This value is relatively small when compared with polymeric membranes tested at pressure above their plasticization pressure. For example, the permeability of unannealed Matrimid membrane increased by more than 40% over a period of 8 h.[50] The normalized permeability seems to be moving gradually into steady state after the 83rd hour.

Sorption Test

The sorption parameters calculated are comparable with previous reports (Table IV). These parameters were determined using linear regression as described in Ref. 43. The coefficients of determination (R^2) were between 0.917 and 0.941. This reflects the close fit between the regression model and the experimental results. The sorption isotherms of CO_2 of the membrane followed the general trend of a concave shape towards the pressure axis as described by the dual-mode sorption model (Figure 16). The dual-mode sorption parameters obtained are shown on Table IV alongside literature values for comparison. The values obtained compare well with literature. Value of $k_D$characterizes the penetrant affinity to be sorbed into the Henry sites of the polymeric membranes. It represents the ease to which the polymer chains in the densely packed matrix can open up to a sufficient size in order to accommodate a gas molecule.[51] Thus, the relatively higher value of k_D is in conformation with its higher solubility as shown in Table II.

CONCLUSION AND RECOMMENDATION

Transport properties and plasticization behaviors of dual-layer membrane prepared from polysulfone were investigated. Morphological as well as permeation, sorption and plasticization properties were evaluated up to a pressure of 50 bar. Results obtained showed that FST can be used to improve the surface morphology of polysulfone composite membrane. Also, the membrane displayed improved plasticization pressure as well as permeability, solubility and diffusion coefficient at plasticization pressure. Overall, lamination of thin top layer of polysulfone prepared from diethylene glycol dimethyl ether on a microporous support prepared from mixture of polysulfone and glycerol in NMP solvent exhibit a potential for high pressure CO_2 removal from natural gas.

ACKNOWLEDGMENTS

The authors gratefully acknowledge the supports of the Membrane Cluster Research Group, Universiti Sains Malaysia, and Center for Petroleum & Minerals, King Fahd University of Petroleum & Minerals, Saudi Arabia.

REFERENCES

1. Baker, R. W.; Lokhandwala, K. *Ind. Eng. Chem. Res.* **2008**, *47*, 2109.
2. Ahmad, A. L.; Adewole, J. K.; Ismail, S. B., Peng, L. C.; Sultan, A. S. Membrane Separation of CO2 from Natural Gas: A State-of-the-Art Review on Material Development; Defect and Diffusion Forum, **2013**; Vol. *333*, p 135.
3. Koros, W. K.; Krotochvil, A.; Shu, S.; Husain, S. Energy and Environmental Issues and Impacts of Membranes in Industry. In Membrane Operations Innovative Separations and Transformations; Drioli, E., Giorno L., Eds.; Wiley-VCH Verlag GmbH & Co. KGaA: Weinheim, **2009**, p 139.
4. Echt, W. I.; Singh, M. Integration of Membranes Into Natural Gas Process Schemes. In UOP LLC, A Honeywell Company, Des Plaines, IL, **2008**.
5. Wijmans, J. G.; Baker, R. W. The Solution–Diffusion Model: A Unified Approach to Membrane Permeation. In Materials Science of Membranes for Gas and Vapor Separation; John Wiley & Sons, Ltd, **2006**; p 159.
6. Julian, H.; Wenten, I. G. *IOSR J. Eng.* **2012**, *2*, 484.
7. Junaidi, M. U. M.; Leo, C. P.; Ahmad, A. L.; Kamal, S. N. M.; Chew, T. L. *Fuel Process. Technol.* **2014**, *118*, 125.
8. Maeda, Y.; Paul, D. R. *J. Polym. Sci., Part B: Polym. Phys.* **1987**, *25*, 957.
9. Kim, H. W.; Park, H. B. *J. Membr. Sci.* **2011**, *372*, 116.
10. Houde, A. Y.; Kulkarni, S. S.; Kulkarni, M. G. *J. Membr. Sci.* **1994**, *95*, 147.
11. McHattie, J. S.; Koros, W. J.; Paul, D. R. *Polymer* **1991**, *32*, 840.
12. McHattie, J. S.; Koros, W. J.; Paul, D. R. *Polymer* **1992**, *33*, 1701.
13. McHattie, J. S.; Koros, W. J.; Paul, D. R. *Polymer* **1991**, *32*, 2618.
14. Ismail, A. F.; Ng, B. C.; Abdul Rahman, W. A. W. *Sep. Purif. Technol.* **2003**; *33*, 255.
15. Bos, A.; Pünt, I. G. M.; Wessling, M.; Strathmann, H. *J. Membr. Sci.* **1999**, *155*, 67.
16. Aroon, M. A.; Ismail, A. F.; Montazer-Rahmati, M. M.; Matsuura, T. *Sep. Purif. Technol.* **2010**, *72*, 194.
17. Scholes, C. A., Chen, G. Q.; Stevens, G. W.; Kentish, S. E. *J. Membr. Sci.* **2010**, *346*, 208.
18. Rafiq, S.; Man, Z.; Maulud, A.; Muhammad, N.; Maitra, S. *J. Membr. Sci.* **2011**, *378*, 444.
19. Iqbal, M.; Man, Z.; Mukhtar, H.; Dutta, B. K. *J. Membr. Sci.* **2008**, *318*, 167.
20. Recio, R.; Palacio, L.; Prádanos, P.; Hernández, A.; Lozano, Á. E.; Marcos, Á.; de la Campa, J. G.; de Abajo, J. *J. Membr. Sci.* **2007**, *293*, 22.

21. Chenar, M. P.; Rajabi, H.; Pakizeh, M.; Sadeghi, M.; Bolverdi, A. *J. Polym. Res.* **2013**, *20*, 216.
22. Wang, D.; Li, K.; Sourirajan, S.; Teo, W. K. *J. Appl. Polym. Sci.* **1993**, *50*, 1693.
23. Moradihamedani, P.; Ibrahim, N. A.; Yunus, W. M. Z. W.; Yusof, N. A. *J. Appl. Polym. Sci.* **2013**, *130*, 1139.
24. Bi, J. J.; Wang, C. L.; Kobayashi, Y.; Ogasawara, K.; Yamasaki, A. *J. Appl. Polym. Sci.* **2003**, *87*, 497.
25. Minoura, N. *J. Appl. Polym. Sci.* **1982**, *27*, 1007.
26. Pfromm, P. H.; Pinnau, I.; Koros, W. J. *J. Appl. Polym. Sci.* **1993**, *48*, 2161.
27. Mousavi, S. A.; Sadeghi, M.; Motamed-Hashemi, M. M. Y.; Pourafshari Chenar, M.; Roosta-Azad, R.; Sadeghi, M. *Sep. Purif. Technol.* **2008**, *62*, 642.
28. Shao, L.; Chung, T.-S.; Wensley, G., Goh, S. H.; Pramoda, K. P. *J. Membr. Sci.* **2004**, *244*, 77.
29. Ismail, A. F.; Lai, P. Y. *Sep. Purif. Technol.* **2003**, *33*, 127.
30. Bos, A. High pressure CO_2/CH_4 separation with glassy polymer membranes: Aspects of CO2-induced plasticization. In Faculty of Chemical Technology, University of Twente, Netherlands, Enschede, **1996**; p 151.
31. Huang, Y.; Paul, D. R. *Ind. Eng. Chem. Res.* **2007**, *46*, 2342.
32. White, L. S.; Blinka, T. A.; Kloczewski, H. A.; Wang, I. F. *J. Membr. Sci.* **1995**, *103*, 73.
33. Jordan, S. M.; Henson, M. A.; Koros, W. J. *J. Membr. Sci.* **1990**, *54*, 103.
34. Li, Y.; Cao, C.; Chung, T. S.; Pramoda, K. P. *J. Membr. Sci.* **2004**, *245*, 53.
35. Li, Y.; Chung, T.-S.; Xiao, Y. *J. Membr. Sci.* **2008**, *325*, 23.
36. Hosseini, S. S.; Peng, N.; Chung, T. S. *J. Membr. Sci.* **2010**, *349*, 156.
37. Jiang, L.; Chung, T.-S.; Li, D. F.; Cao, C.; Kulprathipanja, S. *J. Membr. Sci.* **2004**, *240*, 91.
38. Li, Y.; Chung, T. S. *J. Membr. Sci.* **2010**, *350*, 226.
39. Liu, Y.; Chung, T. S.; Wang, R.; Li, D. F.; Chng, M. L. *Ind. Eng. Chem. Res.* **2003**, *42*, 1190.
40. Adewole, J. K.; Ahmad, A. L.; Ismail, S.; Leo, C. P. *Int. J. Greenh Gas Con.* **2013**, *17*, 46.
41. Merkel, T. C.; Bondar, V.; Nagai, K.; Freeman, B. D.; Yampolskii, P. Y. *Macromolecules* **1999**, *32*, 8427.
42. Ghadimi, A.; Sadrzadeh, M.; Shahidi, K.; Mohammadi, T. *J. Membr. Sci.* **2009**, *344*, 225.
43. Dong, G.; Li, H.; Chen, V. *J. Membr. Sci.* **2011**, *369*, 206.
44. Joly, C.; Le Cerf, D.; Chappey, C.; Langevin, D.; Muller, G. *Sep. Purif. Technol.* **1999**, *16*, 47.
45. Qiu, W.; Chen, C.-C.; Xu, L.; Cui, L.; Paul, D. R.; Koros, W. *J. Macromolecules* **2011**, *44*, 6046.
46. Wind, J. D.; Paul, D. R.; Koros, W. J. *J. Membr. Sci.* **2004**, *228*, 227.
47. Wessling, M.; Schoeman, S.; van der Boomgaard, T.; Smolders, C. A. *Gas Sep. Purif.* **1991**, *5*, 222.
48. Starannikova, L.; Khodzhaeva, V.; Yampolskii, Y. *J. Membr. Sci.* **2004**, *244*, 183.
49. Krantz, W. B.; Greenberg, A. R. Membrane Characterization by Ultrasonic Time-Domain Reflectometry. In Advanced Membrane Technology and Applications; John Wiley & Sons, Inc., Hoboken, New Jersey **2008**; p 879.
50. Bos, A.; Pünt, I. G. M.; Wessling, M.; Strathmann, H. J. Polym. Sci., *Part B: Polym. Phys.* **1998**, *36*, 1547.
51. Vaughn, J. T.; Koros, W. J.; Johnson, J. R.; Karvan, O. *J. Membr. Sci.* **2012**, *401–402*, 163.
52. Wang, J.-S.; Kamiya, Y.; Naito, Y. *J. Polym. Sci., Part B: Polym. Phys.* **1998**, *36*, 1695.